Basic Notions of the 2nd Order Time-Convolution Master Equation

Wenxiang Ying *

August 7, 2024

Contents

*wying3@ur.rochester.edu

1 Theory

1.1 Projection Operator Formalism

For a given Hamiltonian expressed as

$$\hat{H}(t) = \hat{H}_0 + \hat{H}_1(t), \tag{1}$$

where $\hat{H}_0 = \hat{H}_{\rm S} + \hat{h}_{\rm B}$ and $\hat{H}_1(t)$ are the unperturbed part (which consists of the bare system Hamiltonian $\hat{H}_{\rm S}$ and the bare bath Hamiltonian $\hat{h}_{\rm B}$) and the perturbation, respectively. Under the $\hat{H}_0$-interaction picture, the Liouville-von Neumann equation for the total density matrix $\hat{\rho}_I(t)$ is

$$\frac{d}{dt}\hat{\rho}_I(t) = -i\mathcal{L}_I(t)\hat{\rho}_I(t), \tag{2}$$

where $\hat{\rho}_I(t) = \mathcal{G}_0^\dagger(t)\hat{\rho}(t)$, with $\hat{\rho}(t)$ the total density matrix under the Schrödinger picture, and $\mathcal{G}_0(t)$ the free superpropagator. Further, $\mathcal{L}_I(t)\cdot = [\hat{H}_1^I(t), \cdot]$ with $\hat{H}_1^I(t) = \hat{H}_1(t)\mathcal{G}_0^\dagger(t)$. Note that we have chosen $\hbar = 1$ throughout this Note for simplicity.

The system reduced density matrix (RDM) is defined as $\hat{\rho}_{\rm S}(t) := {\rm Tr}_{\rm B}[\hat{\rho}(t)]$, where ${\rm Tr}_{\rm B}[\cdot]$ takes the partial trace over the bath degrees of freedom (DOF). To obtain the dynamics of the RDM, we introduce a projection operator as follows,

$$\mathcal{P}\cdot := \hat{\rho}_{\rm B} \otimes {\rm Tr}_{\rm B}[\cdot], \qquad \mathcal{Q} := 1 - \mathcal{P}. \tag{3}$$

It is straightforward to see that $\mathcal{P}\mathcal{Q} = 0$. And the RDM under the interaction picture can also obtained via $\hat{\rho}_{\rm S}^I(t) = {\rm Tr}_{\rm B}[\mathcal{P}\hat{\rho}_I(t)]$.

With the above definitions, one obtains the following equations of motion,

$$\frac{d}{dt}\mathcal{P}\hat{\rho}_I(t) = -i\mathcal{P}\mathcal{L}_I(t)(\mathcal{P}+\mathcal{Q})\hat{\rho}_I(t), \tag{4}$$

$$\frac{d}{dt}\mathcal{Q}\hat{\rho}_I(t) = -i\mathcal{Q}\mathcal{L}_I(t)(\mathcal{P}+\mathcal{Q})\hat{\rho}_I(t). \tag{5}$$

1.1.1 Time-nonlocal version

Formal integration of Eq. 5 from zero time to t leads to

$$\mathcal{Q}\hat{\rho}_I(t) = -i\int_0^t d\tau\ \exp_+\Big[-i\int_\tau^t ds\ \mathcal{Q}\mathcal{L}_I(s)\Big]\mathcal{Q}\mathcal{L}_I(\tau)\mathcal{P}\hat{\rho}_I(\tau) + \exp_+\Big[-i\int_{t_0}^t d\tau\ \mathcal{Q}\mathcal{L}_I(\tau)\Big]\mathcal{Q}\hat{\rho}_I(0). \tag{6}$$

Plug Eq. 6 into Eq. 4, one obtains

$$\begin{aligned}\frac{d}{dt}\mathcal{P}\hat{\rho}_I(t) = &-i\mathcal{P}\mathcal{L}_I(t)\mathcal{P}\hat{\rho}_I(t) - \mathcal{P}\int_0^t d\tau\ \mathcal{L}_I(t)\exp_+\Big[-i\int_\tau^t ds\ \mathcal{Q}\mathcal{L}_I(s)\Big]\mathcal{Q}\mathcal{L}_I(\tau)\mathcal{P}\hat{\rho}_I(\tau)\\ &- i\mathcal{P}\mathcal{L}_I(t)\exp_+\Big[-i\int_{t_0}^t d\tau\ \mathcal{Q}\mathcal{L}_I(\tau)\Big]\mathcal{Q}\hat{\rho}_I(0),\end{aligned} \tag{7}$$

which can be re-expressed as

$$\begin{aligned}\hat{\rho}_{\rm B}^{\rm eq}\otimes\frac{d}{dt}\hat{\rho}_{\rm S}^{I}(t) = &-i\hat{\rho}_{\rm B}^{\rm eq}\otimes{\rm Tr}_{\rm B}\Big[\mathcal{L}_I(t)\hat{\rho}_{\rm B}^{\rm eq}\Big]\hat{\rho}_{\rm S}^{I}(t)\\ &-\hat{\rho}_{\rm B}^{\rm eq}\otimes{\rm Tr}_{\rm B}\left[\int_0^t d\tau\ \mathcal{L}_I(t)\exp_+\Big[-i\int_\tau^t ds\ \mathcal{Q}\mathcal{L}_I(s)\Big]\mathcal{Q}\mathcal{L}_I(\tau)\hat{\rho}_{\rm B}^{\rm eq}\right]\hat{\rho}_{\rm S}^{I}(\tau)\\ &-i\hat{\rho}_{\rm B}^{\rm eq}\otimes{\rm Tr}_{\rm B}\left[\mathcal{L}_I(t)\exp_+\Big[-i\int_{t_0}^t d\tau\ \mathcal{Q}\mathcal{L}_I(\tau)\Big]\mathcal{Q}\hat{\rho}_I(0)\right].\end{aligned}\tag{8}$$

Taking partial trace over the bath DOF for the above equation leads to

$$\frac{d}{dt}\hat{\rho}_{\rm S}^{I}(t) = -i{\rm Tr}_{\rm B}\Big[\mathcal{L}_I(t)\hat{\rho}_{\rm B}^{\rm eq}\Big]\hat{\rho}_{\rm S}^{I}(t) - \int_0^t d\tau\ \mathcal{K}(t-\tau)\hat{\rho}_{\rm S}^{I}(\tau) + \mathcal{I}(t,0),\tag{9}$$

where the memory kernel $\mathcal{K}(t-\tau)$ is defined as

$$\mathcal{K}(t-\tau) := {\rm Tr}_{\rm B}\left[\mathcal{L}_I(t)\exp_+\Big[-i\int_\tau^t ds\ \mathcal{Q}\mathcal{L}_I(s)\Big]\mathcal{Q}\mathcal{L}_I(\tau)\hat{\rho}_{\rm B}^{\rm eq}\right],\tag{10}$$

captures the effects of the bath on the system over the time interval from 0 to t, reflecting non-Markovian dynamics where the system's history influences its future evolution. Further, the inhomogeneous term $\mathcal{I}(t,0)$ is defined as

$$\mathcal{I}(t,0) := -i{\rm Tr}_{\rm B}\left[\mathcal{L}_I(t)\exp_+\Big[-i\int_{t_0}^t d\tau\ \mathcal{Q}\mathcal{L}_I(\tau)\Big]\mathcal{Q}\hat{\rho}_I(0)\right],\tag{11}$$

which characterizes the influence of the initial state of the bath on the system at time t, which is crucial for accurately describing the system dynamics from an initial condition.

Suppose the system is initialized from a product state, where there is no system-bath correlation at $t=0$ so that the total density matrix is separable, *i.e.*,

$$\hat{\rho}_I(0) = \hat{\rho}(0) = \hat{\rho}_{\rm S}(0)\otimes\hat{\rho}_{\rm B}^{\rm eq},\tag{12}$$

where $\hat{\rho}_{\rm B}^{\rm eq} = e^{-\beta\hat{h}_{\rm B}}/{\rm Tr}_{\rm B}[e^{-\beta\hat{h}_{\rm B}}]$, with $\beta = 1/(k_{\rm B}T)$. As such, $\mathcal{P}\hat{\rho}_I(0) = \hat{\rho}_I(0)$, which results in $\mathcal{Q}\mathcal{P}\hat{\rho}_I(0) = 0$, and the inhomogeneous term defined in Eq. 11 disappear. We further assume a *tricky* identity holds [see Chapter 5, Eq. (5.7) of Ref. [1]]:

$$\mathcal{P}\mathcal{L}_I(t)\mathcal{P} = 0,\tag{13}$$

which can always be satisfied by appropriate denition of $\hat{H}_1(t)$. As such, the first term in the right-hand side of Eq. 9 also disappear, which helps simplify the final expression of Eq. 9 as follows

$$\frac{d}{dt}\hat{\rho}_{\rm S}^{I}(t) = -\int_0^t d\tau\ \mathcal{K}(t-\tau)\hat{\rho}_{\rm S}^{I}(\tau).\tag{14}$$

Eq. 14 is featured in the form of time convolution of a memory kernel with the RDM at an earlier time, known as the *Nakajima-Zwanzig-Mori* formalism, which is formally exact.

The TC approach involves memory effects, where the future state of the system depends on its entire history (Non-Markovian dynamics).

1.2 Second Order Quantum Master Equations

The simplest approximation from the exact formal exact equations are the 2nd order approximations. Let us consider a general form of system-bath coupling Hamiltonian,

$$\hat{H}_1(t) = \sum_a \hat{S}_a(t) \otimes \hat{F}_a(t), \tag{15}$$

where $\hat{S}_a(t)$ and $\hat{F}_a(t)$ are the a-th system and bath dissipation modes, respectively.

1.2.1 Time-nonlocal equation

The time-nonlocal equation can be established from Eq. 14, where the memory kernel defined in Eq. 10 is approximated as

$$\mathcal{K}(t-\tau) \approx \mathcal{K}^{(2)}(t-\tau) := \mathrm{Tr}_{\mathrm{B}}\Big[\mathcal{L}_I(t)\mathcal{L}_I(\tau)\hat{\rho}_{\mathrm{B}}^{\mathrm{eq}}\Big], \tag{16}$$

in which we kept terms only up to the 2nd order. The above approximation is known as the *Born approximation*. Under the interaction picture, the operators are transformed from Heisenberg picture via

$$\hat{H}_1^I(t) = \sum_a \hat{S}_a^I(t) \otimes \hat{F}_a^I(t), \tag{17}$$

where

$$\hat{S}_a^I(t) = \hat{S}_a(t)\mathcal{G}_0^\dagger(t), \qquad \hat{F}_a^I(t) = \hat{F}_a(t)\mathcal{G}_0^\dagger(t). \tag{18}$$

Inserting Eq. 17 into Eq. 16, one obtains

$$\mathcal{K}^{(2)}(t-\tau)\hat{\rho}_I(\tau) = \sum_{a,b} C_{ab}(t-\tau)\Big[\hat{S}_a^I(t), \hat{S}_b^I(\tau)\hat{\rho}_I(\tau)\Big] + \mathrm{h.c.}, \tag{19}$$

where h.c. represents Hermitian conjugate, and the bare-bath time-correlation functions (TCF) are defined as

$$C_{ab}(t-\tau) := \mathrm{Tr}_{\mathrm{B}}\Big[\hat{F}_a^I(t)\hat{F}_b^I(\tau)\hat{\rho}_{\mathrm{B}}^{\mathrm{eq}}\Big]. \tag{20}$$

As a result, the 2nd order time-nonlocal master equation uses Eq. 19 in Eq. 14, reading as

$$\begin{aligned}
\frac{d}{dt}\hat{\rho}_{\mathrm{S}}^I(t) &= -\int_0^t d\tau\ \mathcal{K}^{(2)}(t-\tau)\hat{\rho}_{\mathrm{S}}^I(\tau) \\
&= -\sum_{a,b}\int_0^t d\tau\ C_{ab}(t-\tau)\Big[\hat{S}_a^I(t), \hat{S}_b^I(\tau)\hat{\rho}_I(\tau)\Big] + \mathrm{h.c.} \\
&= -\sum_{a,b}\int_0^t d\tau\ C_{ab}(\tau)\Big[\hat{S}_a^I(t), \hat{S}_b^I(t-\tau)\hat{\rho}_I(t-\tau)\Big] + \mathrm{h.c.},
\end{aligned} \tag{21}$$

where we changed the integration variable as $\tau \to t - \tau$ in the 3rd line. One can further express Eq. 21 under the Schrödinger picture as follows,

$$\frac{d}{dt}\hat{\rho}_{\rm S}(t) = -i[\hat{H}_{\rm S}, \hat{\rho}_{\rm S}(t)] - \sum_{a,b}\int_0^t d\tau \ \Big\{C_{ab}(\tau)\Big[\hat{S}_a, e^{-i\hat{H}_{\rm S}\tau}\hat{S}_b\hat{\rho}_{\rm S}(t-\tau)e^{i\hat{H}_{\rm S}\tau}\Big] \\ - C_{ba}(-\tau)\Big[\hat{S}_a, e^{-i\hat{H}_{\rm S}\tau}\hat{\rho}_{\rm S}(t-\tau)\hat{S}_b e^{i\hat{H}_{\rm S}\tau}\Big]\Big\}. \tag{22}$$

For simplicity, the above equation can be expressed in terms of superoperators as

$$\frac{d}{dt}\hat{\rho}_{\rm S}(t) = -i\mathcal{L}_{\rm S}\hat{\rho}_{\rm S}(t) - \int_0^t d\tau \ \mathcal{K}^{(2)}(\tau)\hat{\rho}_{\rm S}(t-\tau), \tag{23}$$

where the superoperators are defined as

$$\mathcal{L}_{\rm S} \cdot := [\hat{H}_{\rm S}, \ \cdot \ ], \tag{24}$$

$$\begin{aligned}\mathcal{K}^{(2)}(\tau) \cdot &:= \sum_{a,b}\Big\{C_{ab}(\tau)\Big[\hat{S}_a, e^{-i\hat{H}_{\rm S}\tau}\hat{S}_b \ \cdot \ e^{i\hat{H}_{\rm S}\tau}\Big] - C_{ba}(-\tau)\Big[\hat{S}_a, e^{-i\hat{H}_{\rm S}\tau} \ \cdot \ \hat{S}_b e^{i\hat{H}_{\rm S}\tau}\Big]\Big\} \\ &= \sum_{a,b}\Big\{C_{ab}(\tau)\Big[\hat{S}_a e^{-i\hat{H}_{\rm S}\tau}\hat{S}_b \ \cdot \ e^{i\hat{H}_{\rm S}\tau} - e^{-i\hat{H}_{\rm S}\tau}\hat{S}_b \ \cdot \ e^{i\hat{H}_{\rm S}\tau}\hat{S}_a\Big] \\ &\quad - C_{ba}(-\tau)\Big[\hat{S}_a e^{-i\hat{H}_{\rm S}\tau} \ \cdot \ \hat{S}_b e^{i\hat{H}_{\rm S}\tau} - e^{-i\hat{H}_{\rm S}\tau} \ \cdot \ \hat{S}_b e^{i\hat{H}_{\rm S}\tau}\hat{S}_a\Big]\Big\}.\end{aligned} \tag{25}$$

If the bath operators $\hat{F}_a$ are Hermitian, then the bare-bath TCF has time-reversal symmetry, $C_{ba}(-\tau) = C^*_{ab}(\tau)$. Similar to the TCL-2 master equation, one can trivially express Eq. 22 under the adiabatic representation (eigen basis of $\hat{H}_{\rm S}$), which is convenient for the memory kernel construction. But the fact is that the choice of representations will not influence the outcome of the quantum dynamics (same for Redfield).

1.2.2 Finite memory length approximation

In principle, the propagation of the RDM becomes slower as t increases, because the integro-differential equation in Eq. 23 is non-Markovian, which contains memory effects such that the future state of the system depends on its entire history. As t increases, the memory length also increases, making the computational cost grow drastically when trying to obtain the long time dynamics.

Despite the disadvantage, one notices that the memory kernel $\mathcal{K}^{(2)}(\tau)$ decays to zero at the long time limit ($\tau \to \infty$). As a result, one can take the *finite correlation length* approximation, *i.e.*,

$$\frac{d}{dt}\hat{\rho}_{\rm S}(t) = -i\mathcal{L}_{\rm S}\hat{\rho}_{\rm S}(t) - \int_0^{t_{\rm mem}} d\tau \ \mathcal{K}^{(2)}(\tau)\hat{\rho}_{\rm S}(t-\tau), \tag{26}$$

where $t_{\rm mem}$ is the memory length, serving as the upper bound of the integration, which greatly reduce the computational cost at the long time regime (where $t \gg t_{\rm mem}$). Note that in the short time regime when $t < t_{\rm mem}$, one shall still use Eq. 23 (with t the upper bound of integration) to propagate the dynamics to ensure $t - \tau \geq 0$. Note that $t_{\rm mem}$ can also be viewed as a convergence control parameter, and the choice of $t_{\rm mem}$ usually depends on the characteristic timescale of the bath TCF.

1.2.3 Remarks on numerical implementation, and properties

1, Construction of the memory kernel. Unlike the non-Markovian Redfield equation where the Redfield tensor needs to be updated on-the-fly (because it contains time integration), the memory kernel can be directly obtained according to Eq. 25 before the dynamics starts, and is fixed during the propagation of the RDM. As a result, one just needs to initialize the memory kernel from $t = 0$ to t_{mem}, which will be used to calculate the tensor-matrix products within the memory length.

2, Propagation of the dynamics. With the memory kernel, one faces with the situation to solve the Volterra integro-differential equation (IDE) in Eq. 23. However, the conventional RK-4 integrator cannot be directly implemented. The RK-4 integrator for this type of IDE can be found in Refs. [2, 3]. Nevertheless, one can still use the conventional RK-4 integrator for the coherent part (Schrödinger dynamics), and treat the relaxation term (with carries integration on the memory kernel) simply via Euler integrator (but less accurate and less stable).

3, Properties of the TNL-2 master equation. Similar to the Redfield equation, the TNL-2 master equation is usually trace-preserving. Specifically, the Hamiltonian part of the equation naturally preserves the trace, and the nonlocal integral term's contribution to trace preservation depends on the properties of the memory kernel, *i.e.*, if the memory kernel is designed to describe physically valid processes that conserve probability, then the trace of the RDM is preserved. Furthermore, the TNL-2 master equation correctly produce a thermalized state for asymptotic propagation, but does not guarantee a positive time evolution of the density matrix. The TNL-2 master equation approaches the correct dynamics for sufficiently weak coupling to the environment.

4, Comparison with the Redfield equation. The non-Markovian Redfield equation is time local (also known as TCL-2 master equation), being more efficient in propagation. But it fails under the high temperature regime or with a highly non-Markovian bath. Reichman, *et al.* [4] had provided an estimator that characterizes the accuracy of Redfield theory, $\eta = \max[2\lambda/(\beta\omega_{\mathrm{c}}^2), 2\lambda/(\pi\omega_{\mathrm{c}})]$, where λ is the reorganization energy, ω_{c} is the bath characteristic frequency. Redfield theory becomes unreliable when $\eta > 1$. More details about the non-Markovian Redfield equation can be found at `https://github.com/Okita0512/Non-Markovian-Redfield`. On the other hand, although the TNL-2 master equation highlights non-Markovian effect, which reduces to the TCL-2 master equation under the Markovian approximation upon the RDM, it is not necessarily true that TNL-2 always outperforms TCL-2 [1], even for certain types of highly non-Markovian models. The results highly depends on the bath Hamiltonian as well as its coupling to the system. Details can be found in the numerical results presented later.

4, More. It is well-known that the TNL-2 master equation is theoretically equivalent to the hierarchical equations of motion (HEOM) [5, 6, 7, 8] with only one tier (which is also known as the *chronological time ordering* approximation, COP) [7]. More generally, the HEOM approach with n tiers are proved to be equivalent to the $2n$-th order perturbative master equation [9, 10, 11]. However, the numerical results might differ due to many details, such as the way to obtain the bath TCF, numerical properties associated with the propagator, *etc.* Examples are shown later.

2 Numerical Examples

In this section, we provide a bunch of numerical results of the TNL-2 master equation for several typical model systems. The code implemented in these numerical calculations are available at `https://github.com/Okita0512/TNL-2-Master-Equation`.

2.1 The Spin-Boson Model

The spin-boson model Hamiltonian reads as follows,

$$\hat{H} = \epsilon\hat{\sigma}_z + \Delta\hat{\sigma}_x + \frac{1}{2}\sum_j \omega_j(\hat{x}_j^2 + \hat{p}_j^2) + \hat{\sigma}_z \otimes \hat{F}, \qquad \hat{F} \equiv \sum_j c_j\hat{x}_j. \tag{27}$$

According to the Caldeira-Leggett model, the bath as well as its interacting with the system can be described by the spectral density function, defined as follows,

$$J(\omega) \equiv \frac{1}{2}\int_{-\infty}^{+\infty} dt\ e^{i\omega t}\langle[\hat{F}(t), \hat{F}(0)]\rangle_{\mathrm{B}} = \frac{\pi}{2}\sum_{j=1}^{N}\frac{c_j^2}{\omega_j}\delta(\omega - \omega_j). \tag{28}$$

The reduced system is initially prepared on the excited state, *i.e.*, $\hat{\rho}_{\mathrm{S}}(0) = |e\rangle\langle e|$, and the bath is initially a thermal equilibrium state and decoupled from the system DOF, see Eq. 12.

2.1.1 Ohmic spectral density

The commonly used spectral density function is of the Ohmic form with exponential cutoff,

$$J(\omega) = \frac{\pi}{2}\alpha\omega e^{-\omega/\omega_{\mathrm{c}}}, \tag{29}$$

where α is the Kondo parameter, and ω_{c} is the bath characteristic frequency. The bare-bath TCF needs to be properly discretized. Here we adopt the following strategy,

$$\omega_j = -\omega_{\mathrm{c}}\ln[1 - j/(1 + N_b)], \qquad j = 1, \cdots, N_b, \tag{30a}$$

$$c_j = \sqrt{\frac{\alpha\omega_{\mathrm{c}}}{N_b + 1}}\omega_j, \qquad j = 1, \cdots, N_b, \tag{30b}$$

and N_b is the number of bath oscillators. A number of numerical results are presented and compared to the TCL-2 master equation (Redfield), see Fig. 1 for details.

2.1.2 Debye spectral density

Another type of cutoff function for the Ohmic spectral density is the Lorentzian cutoff, known as the Debye spectral density or the Drude-Lorentz model, which is the overdamped limit of the Brownian oscillator. The Debye spectral density reads as follows,

$$J(\omega) = \frac{2\lambda\omega_{\mathrm{c}}\omega}{\omega^2 + \omega_{\mathrm{c}}^2}, \tag{31}$$

where λ is the reorganization energy, and ω_c is the bath characteristic frequency. One commonly used type of bath discretization procedure is described as follows,

$$\omega_j = \omega_c \tan\left[\frac{\pi}{2}\left(1 - \frac{j}{N_b+1}\right)\right], \qquad j = 1, \cdots, N_b, \tag{32a}$$

$$c_j = \sqrt{\frac{2\lambda}{N_b+1}}\omega_j, \qquad j = 1, \cdots, N_b, \tag{32b}$$

and N_b is the number of bath oscillators. A number of numerical results are presented and compared to the TCL-2 master equation (Redfield), as well as the HEOM with one tier, see Fig. 2 for details. Theoretically, the TNL-2 master equation is equivalent to the HEOM with only one tier. The numerical results show overall accordance between them, but minor discrepancies are also exhibited (for example, Model 19). This could be numerical issues such as the bath discretization, the propagator, *etc.*, which remain to be explored.

2.2 Photon Echoes

Consider a two-level atom coupled to an optical cavity, whose Hamiltonian can be expressed as follows,

$$\hat{H} = \hat{H}_S + \hat{h}_B + \hat{H}_{SB}, \tag{33}$$

where

$$\hat{H}_S := \epsilon_1|1\rangle\langle 1| + \epsilon_2|2\rangle\langle 2|, \tag{34}$$

$$\hat{h}_B := \frac{1}{2}\sum_{j=1}^{N}(\hat{p}_j^2 + \omega_j^2\hat{x}_j^2), \tag{35}$$

$$\hat{H}_{SB} := \mu_0(|1\rangle\langle 2| + |2\rangle\langle 1|) \otimes \sum_{j=1}^{N}\omega_j\lambda_j(r_0)\hat{x}_j, \tag{36}$$

where $\epsilon_1 = -0.6738$, $\epsilon_2 = -0.2798$ are the energy levels of the atom, and the transition dipole moment $\mu_0 = -1.034$ (all in atomic units). $\hat{h}_B$ represents the optical field part, where the frequency of the j-th mode is $\omega_j = j\pi c/L$, where $c = 137.036$ is the speed of light in vacuum (in a.u.), and L is the volume length of the cavity. Furthermore, the atom-field interaction strength reads as

$$\lambda_j(r_0) := \sqrt{\frac{2}{\epsilon_0 L}}\sin\left(\frac{j\pi r_0}{L}\right), \qquad j = 1, \cdots, N, \tag{37}$$

where $\epsilon_0 = 1/(4\pi)$ is the vacuum permittivity (in a.u.), and r_0 is the location of the atom. Here the parameters are taken as $L = 236200$ a.u., and $r_0 = L/2$. The maximum number of standing-wave cavity modes is taken as $N = 400$, which ensures convergence.

This model is widely studied with various quantum dynamics methods, for example, see Refs. [12, 13, 14, 15]. The photon echo is an extreme example of non-Markovian effect of the bath, which is intrinsically the Poincaré recurrence. This effect is well-captured by the TNL-2 master equation, while failed to be described by the TCL-2 master equation. See Fig. 3 for details.

References

[1] Seogjoo J. Jang. 5 - quantum dynamics of molecular excitons. In Seogjoo J. Jang, editor, *Dynamics of Molecular Excitons*, Nanophotonics, pages 107–147. Elsevier, 2020.

[2] Ch. Lubich. Runge-Kutta theory for Volterra integrodifferential equations. *Numerische Mathematik*, 40(1):119, 02 1982.

[3] Yifan Lai and Eitan Geva. On simulating the dynamics of electronic populations and coherences via quantum master equations based on treating off-diagonal electronic coupling terms as a small perturbation. *The Journal of Chemical Physics*, 155(20):204101, 11 2021.

[4] Andrés Montoya-Castillo, Timothy C. Berkelbach, and David R. Reichman. Extending the applicability of Redfield theories into highly non-Markovian regimes. *The Journal of Chemical Physics*, 143(19):194108, 11 2015.

[5] Yoshitaka Tanimura. Nonperturbative expansion method for a quantum system coupled to a harmonic-oscillator bath. 41:6676–6687, Jun 1990.

[6] Yoshitaka Tanimura. Stochastic liouville, langevin, fokker–planck, and master equation approaches to quantum dissipative systems. 75(8):082001, 2006.

[7] Rui-Xue Xu, Ping Cui, Xin-Qi Li, Yan Mo, and YiJing Yan. Exact quantum master equation via the calculus on path integrals. 122(4):041103, 2005.

[8] Rui-Xue Xu and YiJing Yan. Dynamics of quantum dissipation systems interacting with bosonic canonical bath: Hierarchical equations of motion approach. 75:031107, Mar 2007.

[9] Markus Schröder, Michael Schreiber, and Ulrich Kleinekathöfer. Reduced dynamics of coupled harmonic and anharmonic oscillators using higher-order perturbation theory. 126(11):114102, 03 2007.

[10] Liping Chen, Renhui Zheng, Qiang Shi, and YiJing Yan. Optical line shapes of molecular aggregates: Hierarchical equations of motion method. 131(9):094502, 09 2009.

[11] Hao Liu, Lili Zhu, Shuming Bai, and Qiang Shi. Reduced quantum dynamics with arbitrary bath spectral densities: Hierarchical equations of motion based on several different bath decomposition schemes. 140(13):134106, 2014.

[12] Norah M. Hoffmann, Christian Schäfer, Angel Rubio, Aaron Kelly, and Heiko Appel. Capturing vacuum fluctuations and photon correlations in cavity quantum electrodynamics with multitrajectory ehrenfest dynamics. *Phys. Rev. A*, 99:063819, Jun 2019.

[13] Norah M. Hoffmann, Christian Schäfer, Niko Säkkinen, Angel Rubio, Heiko Appel, and Aaron Kelly. Benchmarking semiclassical and perturbative methods for real-time simulations of cavity-bound emission and interference. *The Journal of Chemical Physics*, 151(24):244113, 12 2019.

[14] Tao E. Li, Hsing-Ta Chen, Abraham Nitzan, and Joseph E. Subotnik. Quasiclassical modeling of cavity quantum electrodynamics. *Phys. Rev. A*, 101:033831, Mar 2020.

[15] Maximilian A. C. Saller, Aaron Kelly, and Eitan Geva. Benchmarking quasiclassical mapping hamiltonian methods for simulating cavity-modified molecular dynamics. *The Journal of Physical Chemistry Letters*, 12(12):3163–3170, 2021.

[16] Xin He and Jian Liu. A new perspective for nonadiabatic dynamics with phase space mapping models. *The Journal of Chemical Physics*, 151(2):024105, 07 2019.

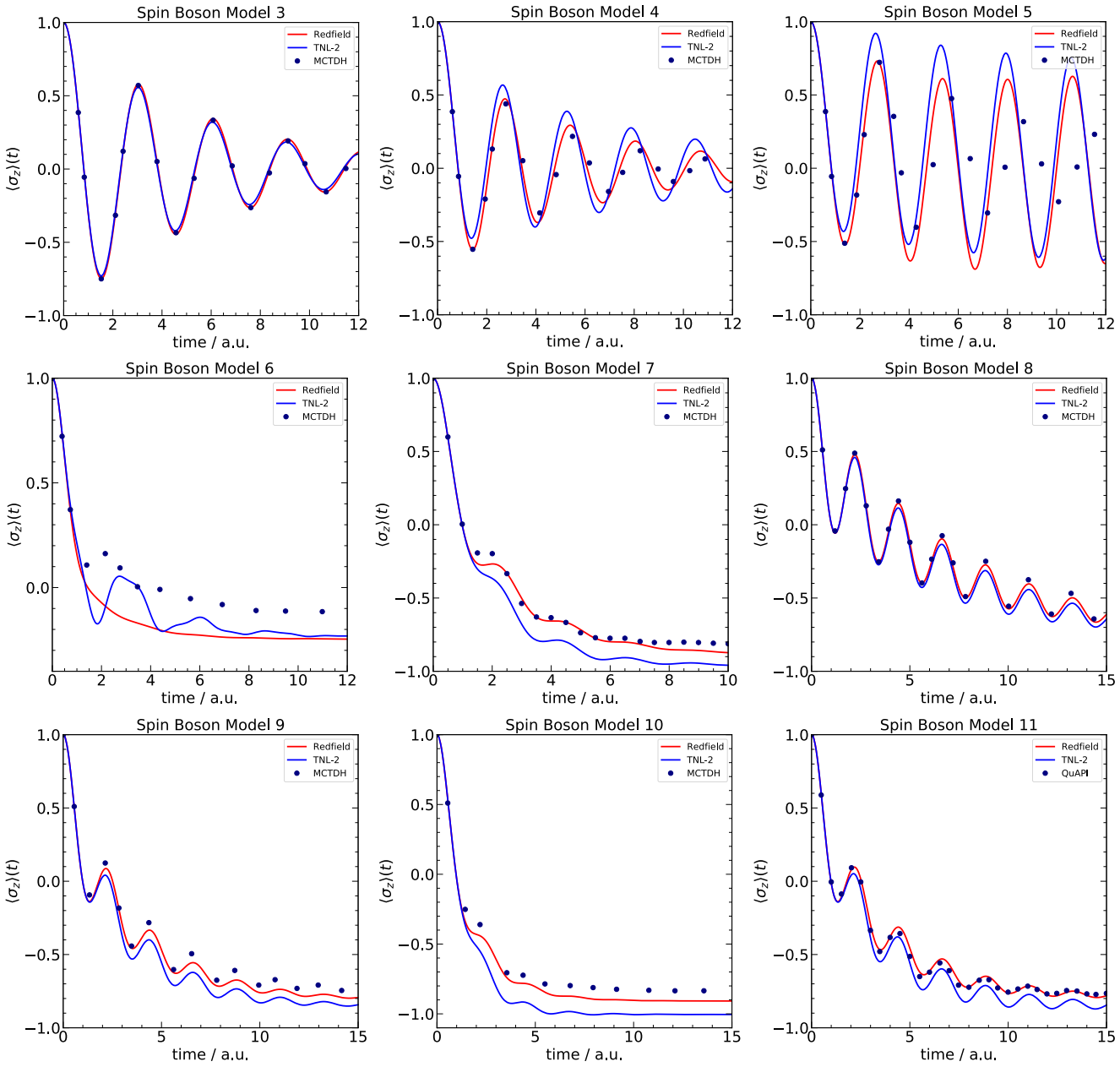

Figure 1: Numerical results of the spin-boson model with Ohmic spectral density. The models are taken from Ref. [16] with orginal labeling. Results are compared with the numerically exact MCTDH or QuAPI. The model parameters are as follows.

(a) Model 3: $\epsilon = 0,\ \Delta = 1,\ \beta = 0.25,\ \omega_c = 5,\ \alpha = 0.02$;
(b) Model 4: $\epsilon = 0,\ \Delta = 1,\ \beta = 0.25,\ \omega_c = 1,\ \alpha = 0.1$;
(c) Model 5: $\epsilon = 0,\ \Delta = 1,\ \beta = 0.25,\ \omega_c = 0.25,\ \alpha = 0.4$;
(d) Model 6: $\epsilon = 1,\ \Delta = 1,\ \beta = 0.25,\ \omega_c = 1,\ \alpha = 0.4$;
(e) Model 7: $\epsilon = 1,\ \Delta = 1,\ \beta = 5,\ \omega_c = 2,\ \alpha = 0.4$;
(f) Model 8: $\epsilon = 1,\ \Delta = 1,\ \beta = 5,\ \omega_c = 2.5,\ \alpha = 0.1$;
(g) Model 9: $\epsilon = 1,\ \Delta = 1,\ \beta = 5,\ \omega_c = 2.5,\ \alpha = 0.2$;
(h) Model 10: $\epsilon = 1,\ \Delta = 1,\ \beta = 5,\ \omega_c = 2.5,\ \alpha = 0.4$;
(i) Model 11: $\epsilon = 1,\ \Delta = 1,\ \beta = 10,\ \omega_c = 2.5,\ \alpha = 0.2$.

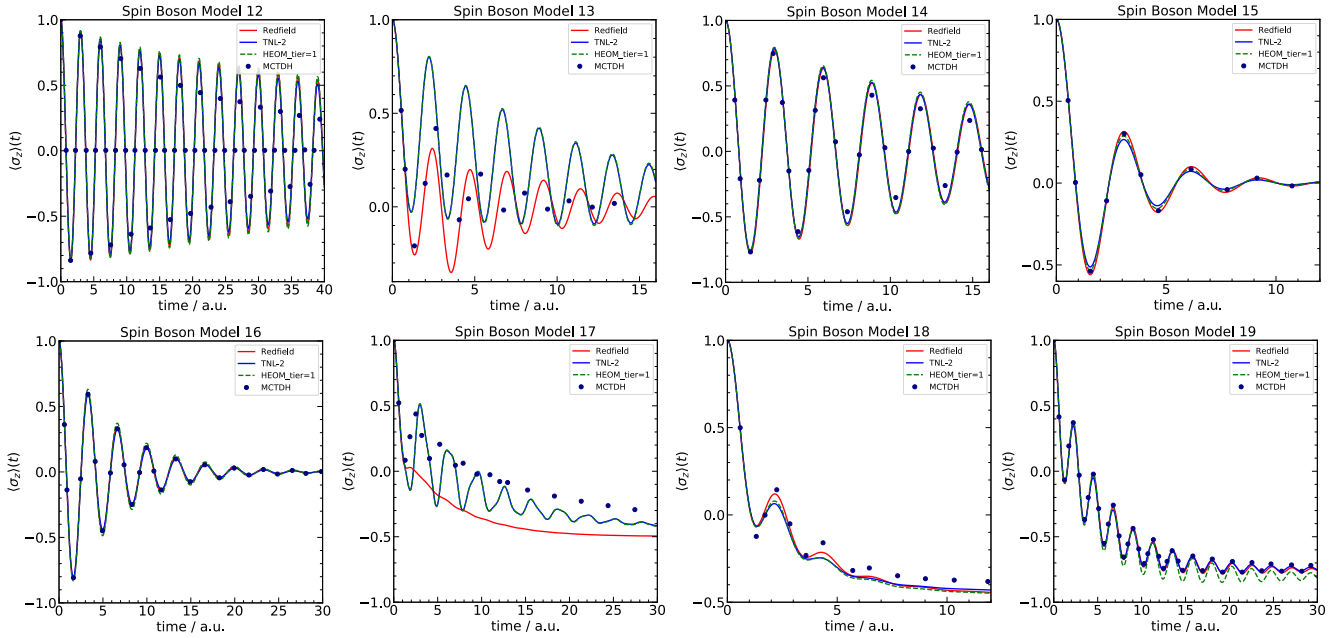

Figure 2: Numerical results of the spin-boson model with Debye spectral density. The models are taken from Ref. [16] with orginal labeling. Results are compared with the numerically exact MCTDH. The model parameters are as follows.

(a) Model 12: $\epsilon = 0,\ \Delta = 1,\ \beta = 0.5,\ \omega_c = 0.25,\ \lambda = 0.025$;
(b) Model 13: $\epsilon = 0,\ \Delta = 1,\ \beta = 0.5,\ \omega_c = 0.25,\ \lambda = 0.25$;
(c) Model 14: $\epsilon = 0,\ \Delta = 1,\ \beta = 5,\ \omega_c = 0.25,\ \lambda = 0.25$;
(d) Model 15: $\epsilon = 0,\ \Delta = 1,\ \beta = 0.5,\ \omega_c = 5,\ \lambda = 0.25$;
(e) Model 16: $\epsilon = 0,\ \Delta = 1,\ \beta = 50,\ \omega_c = 5,\ \lambda = 0.25$;
(f) Model 17: $\epsilon = 1,\ \Delta = 1,\ \beta = 0.5,\ \omega_c = 0.25,\ \lambda = 0.25$;
(g) Model 18: $\epsilon = 1,\ \Delta = 1,\ \beta = 0.5,\ \omega_c = 5,\ \lambda = 0.25$;
(h) Model 19: $\epsilon = 1,\ \Delta = 1,\ \beta = 50,\ \omega_c = 5,\ \lambda = 0.25$.

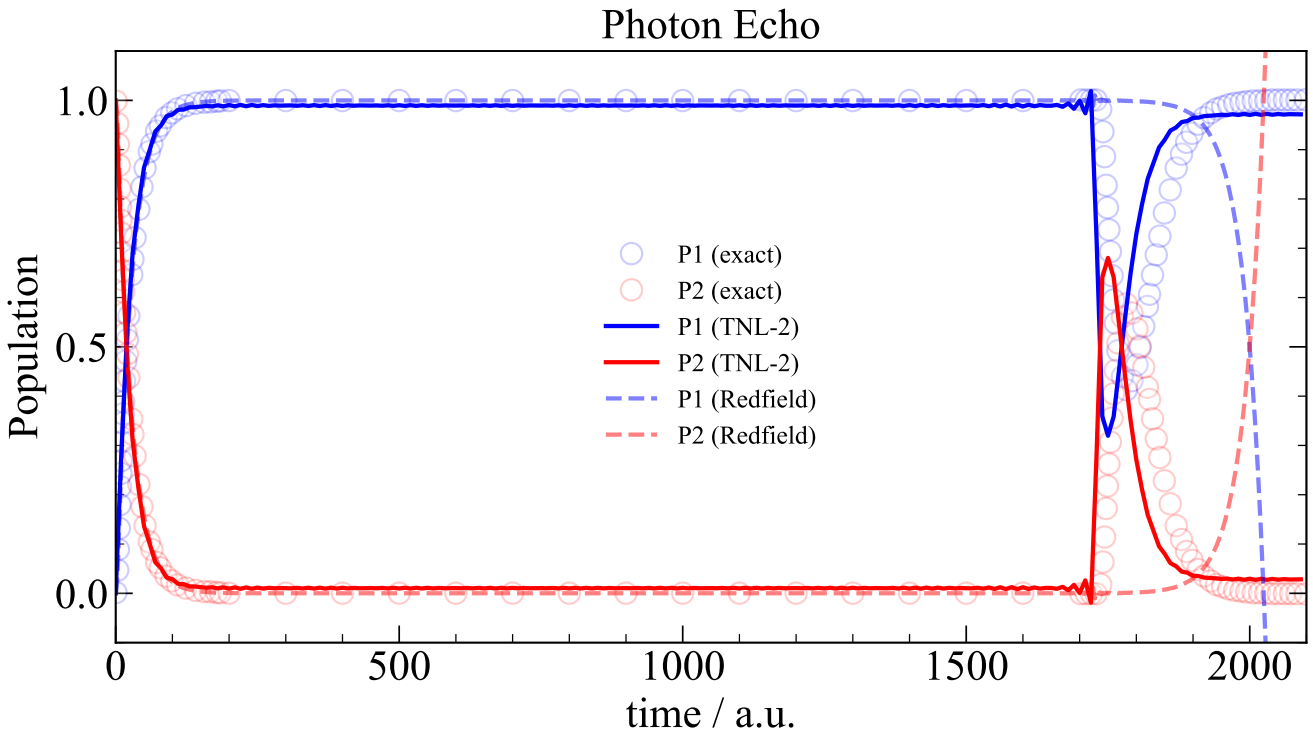

Figure 3: Numerical results of the population dynamics for two-level atom in a cavity model. P1 and P2 represents the population of the ground and excited state of the atom, respectively. The TNL-2 master equation results (with full memory length, integration time step $dt = 0.1$) are in solid lines, the Redfield equation results are in dashed lines, and the numerically exact results are in open circles for comparison.